J. Fluid Mech. (1989), *vol.* 204, *pp.* 457–478
Printed in Great Britain

Further experiments on the evolution of turbulent stresses and scales in uniformly sheared turbulence

By S. TAVOULARIS AND U. KARNIK
Department of Mechanical Engineering, University of Ottawa, Ottawa, Canada K1N 6N5

(Received 13 April 1987 and in revised form 23 January 1989)

Measurements of the Reynolds stresses, integral lengthscales and Taylor microscales are reported for several cases of uniformly sheared turbulent flows with shear values in a range substantially wider than those of previous measurements. It is shown that such flows demonstrate a self-preserving structure, in which the dimensionless Reynolds stress ratios and the dissipation over production ratio, ϵ/P, remain essentially constant. Flows with sufficiently large $k_s = (1/\overline{U}_c)\mathrm{d}\overline{U}_1/dx_2$ have exponentially growing stresses and $\epsilon/P \approx 0.68$; a linear relationship between the coefficient in the exponential law and k_s is shown to be compatible with measurements having $k_s > 3$. The possibility of a self-preserving structure with asymptotically constant stresses and $\epsilon/P \approx 1.0$ is also compatible with measurements, corresponding to flows with small values of k_s. The integral lengthscales appear to grow according to a power law with an exponent of about 0.8, independent of the mean shear, while the Taylor microscales, in general, approach constant values. Various attempts to scale the stresses and to predict their evolution are discussed and the applicability of Hasen's theory is scrutinized. Finally, an 'exact' expression for the pressure–strain rate covariance is derived and compared to some popular models.

1. Introduction

The concept of homogeneous turbulence subjected to a uniform mean shear has long attracted the attention of turbulence researchers, being a popular paradigm in the development and verification of turbulence theories.

Analyses and computations concerning various aspects of such flows have been published by many investigators, including Reis (1952), Burgers & Mitchner (1953), Tchen (1953), Craya (1958), Deissler (1961, 1965, 1970), Fox (1964), Hasen (1967), Shaanan, Ferziger & Reynolds (1977), Corrsin & Kollman (1977), Gence, Angel & Mathieu (1978), Courseau & Loiseau (1978), Rogallo (1981), Cambon, Jeandel & Mathieu (1981), Feiereisen *et al.* (1982), Rogallo & Moin (1984), Moin, Rogers & Moser (1985) and Tavoularis (1985). Since Corrsin's (1963) initial suggestions for an experimental realization, flows with approximately uniform shear and transverse homogeneity have been generated in the laboratory by Rose (1966, 1970), Robertson & Johnson (1970), Champagne, Harris & Corrsin (1970), Hwang (1971), Mulhearn & Luxton (1975), Harris, Graham & Corrsin (1977), Tavoularis & Corrsin (1981*a*, *b*), Karnik (1983), Karnik & Tavoularis (1983), Sreenivasan (1985) and Rohr *et al.* (1988). The available experimental studies were meant to approximate unbounded flows with constant shear. However, the finite size of wind tunnels, both in cross-section and in length, as well as the imposed geometry of the flow generator are factors limiting the validity of this analogy.

Previous analyses and experiments have contributed to our understanding of the

influence of mean shear on the structure of turbulence. At the same time, it has become evident that uniformly sheared turbulent flows have their own distinct characteristics and that, perhaps, they deserve to be treated as a class. The possibility of subdividing this class according to some criterion also requires attention. Thus, one should be interested in resolving whether, for a given apparatus and upstream conditions, the turbulence structure would approach a self-preserving state and, if indeed a self-preserving state is reached, whether it would be universal or particular to a subclass of flows, distinct from the others.

The objectives of the present study are to expand the range of available measurements and to re-evaluate earlier results in an attempt to provide a unified view of uniformly sheared turbulence.

2. Measurements

2.1. *Experimental facility*

The wind tunnel and related apparatus that were used in the present experiments have been described by Karnik & Tavoularis (1987). The air flow was produced by two centrifugal blowers and passed through a filter, a honeycomb, a settling chamber with several turbulence-reducing screens and a 16:1 rectangular contraction before entering the final section which had a height $h = 0.305$ m. The sidewalls were about 0.45 m apart and were adjusted for boundary-layer compensation.

The desired mean velocity profile was produced with the use of a shear generator inserted in the flow immediately following the contraction. It consisted of 12 parallel channels, each with a height $M = 25.4$ mm and containing a number of screens selected to produce the desired pressure drop. To obtain uniformity of scales, the flow was directed through a flow separator, consisting of 12 channels, aligned with these in the shear generator. The test section also permitted the insertion of up to four frames containing either grids of parallel cylindrical rods (with solidity $\sigma = 0.378$) or square-mesh woven gauzes ($0.26 < \sigma < 0.45$). The spacing, M_g, between the grid or screen elements varied between 1.6 and 50.8 mm. The grids and screens were tested in a uniform flow and those which imparted significant non-uniformities to the mean and/or turbulent fields were discarded.

The fluctuating velocity was measured with conventional hot-wire anemometers; digital data acquisition and processing was done using a microcomputer.

2.2 *The mean shear*

Detailed measurements published earlier (Karnik & Tavoularis 1987) have demonstrated that the shear generator produced a mean velocity field with a uniform gradient which was preserved in the core of the entire test section and also exhibited fair spanwise uniformity. Insertion of one or more screens reduced the oncoming shear by a factor depending on the screen geometry. In all cases presented here, the mean velocity downstream of screens was found to be unidirectional, with an essentially uniform transverse gradient.

2.3. *The development of the Reynolds stresses*

As shown in figure 1 for a few typical cases, the r.m.s. turbulent velocities presented a mild transverse non-uniformity that was comparable with or lower than those in earlier experiments. Following the practice introduced by Harris *et al.* (1977), the

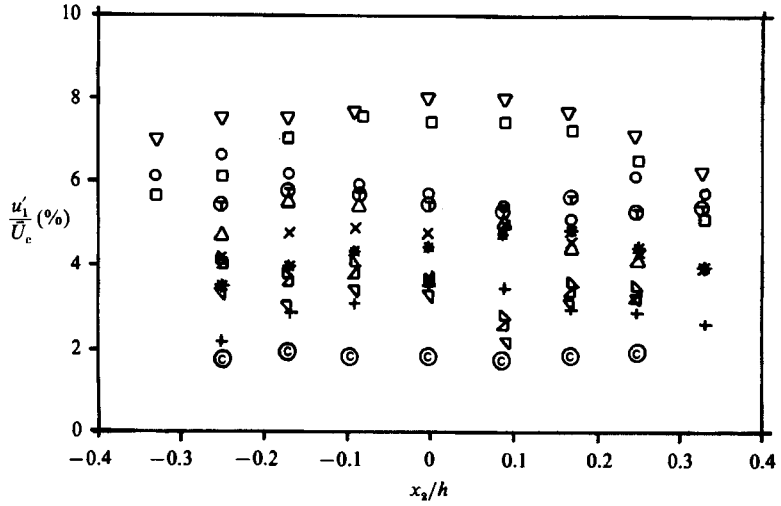

FIGURE 1. Typical transverse variation of the streamwise r.m.s. velocity fluctuations. Symbols as in table 1. $x_1/h = 7.5$ (○, □, ▽); 8.3 (△, ◺, ◹, ◿); 10.0 (ⓒ); 11.0 (Ⓣ); 11.7 (×, +, *).

downstream development of the turbulent characteristics will be plotted versus the total strain

$$\tau = \frac{x_1 - x_g}{\bar{U}_c} \frac{\mathrm{d}\bar{U}_1}{\mathrm{d}x_2}, \tag{1}$$

where $\bar{U}_c$ is the centreline mean speed, x_1 is the distance from the exit of the flow separator and x_g is the downstream position of the grid, where applicable. A summary of the experimental conditions and some reference values of the measured quantities are presented in table 1.

The development of the four dominant Reynolds stresses and the turbulent kinetic energy $\overline{q^2} = \overline{u_i u_i}$ along the wind-tunnel axis is shown in figure 2 for some representative conditions; semilogarithmic coordinates were used for convenient comparison with Tavoularis's (1985) predictions. In all cases, the plots demonstrated linear ranges with either positive or nearly zero slopes, corresponding to either exponential growth or constancy of the Reynolds stresses. For each set of conditions, the rates of growth of all stresses away from the origin were essentially the same. The magnitudes of the stresses were always ordered as $\overline{u_1^2} > \overline{u_3^2} > \overline{u_2^2} < |\overline{u_1 u_2}|$. The same ordering has been observed by others in uniformly sheared flows as well as in inhomogeneous flows with a fixed dominant mean shear direction. The first inequality reflects the fact that the streamwise normal stress receives energy directly from the mean shear, while the other two normal stresses are maintained by means of their coupling to the streamwise stress through pressure–velocity correlations (Champagne *et al.* 1970). Plots of the ratios $\overline{u_i u_i}/(\bar{U}_c^2)$, corresponding to the same flow generating apparatus but different $\bar{U}_c$, essentially collapse when plotted versus the total strain (see also Rohr *et al.* 1988).

All present and some previous measurements of the turbulent kinetic energy are summarized in figure 3. Each set of data away from the origin was fitted by the relation (Tavoularis 1985)

$$\overline{q^2} = \overline{q_r^2}\, \mathrm{e}^{k(x_1 - x_r)}, \tag{2}$$

where x_r, $\overline{q_r^2}$ are reference values, corresponding to a location near the end of the wind tunnel, and k has dimensions of a wavenumber. Based on the least-squares-fitted

Case and symbol	M (mm)	M_g (mm)	σ_g	x_g/h	x_r/h	$\overline{U_c}$ (m/s)	$d\overline{U_1}/dx_2$ (s^{-1})	$\overline{q_r^2}$ (m^2/s^2)	K_{11}	K_{22}	K_{33}	$-K_{12}$	L_{11} (mm)	λ_{11} (mm)	$R_{\lambda 1}$
A ○	25.4	—	—	—	10	13	84	1.714	0.55	0.20	0.25	0.165	38	4.9	310
B ◐	25.4	—	—	—	10	9	60	0.912	0.56	0.20	0.24	0.165	37	—	—
C ●	25.4	—	—	—	10	6	43.5	0.490	0.59	0.19	0.22	0.165	42	—	—
D □	25.4	25.4	0.378	4.5	10	13	38.4	1.422	0.53	0.20	0.27	0.170	50	6.4	360
E ◧	25.4	25.4	0.378	4.5	10	9	28	0.684	0.55	0.20	0.25	0.170	48	—	—
F ■	25.4	25.4	0.378	4.5	10	6	18.4	0.264	0.58	0.19	0.23	0.170	41	—	—
G △	25.4	12.7	0.378	1.1	10	13	39.9	0.997	0.49	0.22	0.29	0.148	50	5.8	270
H ◺	25.4	12.7	0.294	1.1	10	13	50.3	0.446	0.49	0.21	0.30	0.148	30	3.9	120
I ◹	25.4	3.18	0.294	1.1	10	13	43.7	0.344	0.49	0.22	0.29	0.158	26	5.1	140
J ◿	25.4	1.59	0.294	1.1	10	13	48.8	0.419	0.49	0.23	0.28	0.154	26	5.2	160
K *	25.4	1.59	0.294	1.1	10	13	20.9	0.687	0.48	0.24	0.28	0.149	—	—	—
	—	25.4	0.378	4.5	—	—	—	—	—	—	—	—	—	—	—
L ▽	25.4	50.8	0.378	1.1	10	13	29	2.230	0.52	0.22	0.26	0.155	92	6.1	440
M ▼	25.4	50.8	0.378	1.1	10	9	20	0.978	0.55	0.21	0.24	0.155	87	—	—
N ▼	25.4	50.8	0.378	1.1	10	6	13.4	0.388	0.57	0.19	0.24	0.155	87	—	—
O ×	25.4	50.8	0.378	1.1	10	13	13.6	0.914	0.45	0.24	0.31	0.148	—	—	—
	—	25.4	0.378	4.5	—	—	—	—	—	—	—	—	—	—	—
P +	25.4	50.8	0.378	1.1	10	13	9.0	0.437	0.45	027	0.28	0.178	—	—	—
	—	25.4	0.378	2.5	—	—	—	—	—	—	—	—	—	—	—
	—	12.7	0.378	4.5	—	—	—	—	—	—	—	—	—	—	—
R0 (R)	var	—	—	—	10	15.4	13.7	0.065	0.44	0.26	0.30	0.16	38	10.5	20
R1 (R)	6.4	—	—	—	9	15.2	12.2	0.0046	—	—	—	—	—	—	—
R2 (R)	6.4	8.5	0.342	0.25	9	15.2	8.8	0.011	—	—	—	—	—	—	—
R3 (R)	6.4	12.7	0.347	0.25	9	15.2	8.9	0.023	—	—	—	—	—	—	—
R4 (R)	6.4	25.4	0.348	0.25	9	15.2	—	8.8	0.043	—	—	—	—	—	—
R5 (R)	6.4	50.8	0.348	0.25	9	15.2	9.3	0.13	—	—	—	—	—	—	—
CHC (C)	25.4	—	—	—	10	12.2	12.9	0.098	0.47	0.25	0.28	0.165	48	10.9	155
ML (M)	var.	6.4	hon.	—	9	4.6	5.5	0.045	0.48	0.22	0.30	0.18	22	16.0	155
TC (T)	30.5	—	—	—	10	12.4	46.8	0.765	0.53	0.19	0.28	0.14	51	5.8	245
S1 (S1)	30.5	15.2	0.31	0.10	10	0.20	1.23	0.00060	—	—	—	—	50	10.0	101
S2 (S2)	30.5	15.2	0.31	0.10	10	0.20	0.96	0.00036	—	—	—	—	50	10.0	124
S3 (S3)	30.5	15.2	0.31	0.10	10	0.26	1.29	0.00060	—	—	—	—	—	—	—
S4 (S4)	30.5	—	0.31	0.10	10	0.20	1.13	0.00066	—	—	—	—	—	—	—
S5 (S5)	15.2	38.1	0.31	0.03	10	0.28	1.30	0.00133	—	—	—	—	—	—	—
S6 (S6)	15.2	38.1	0.31	0.30	10	0.28	1.21	0.00066	—	—	—	—	—	—	—

TABLE 1. Summary of measurements. References: A–P, present measurements; R0, Rose (1966); R1–R5, Rose (1970); CHC, Champagne *et al.* (1970); ML, Mulhearn & Luxton (1975); TC, Tavoularis & Corrsin (1981*a*); S1–S6, Rohr *et al.* (1988).

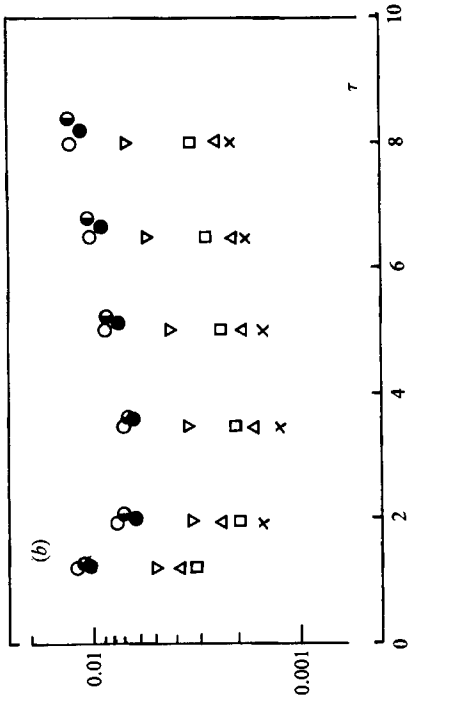

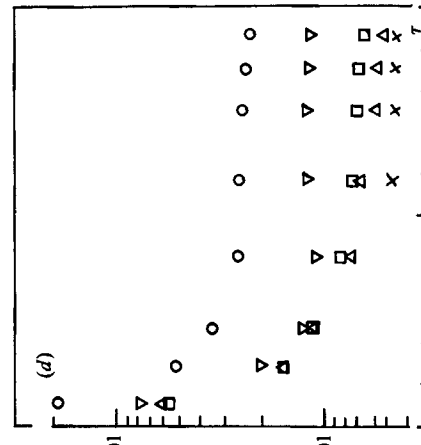

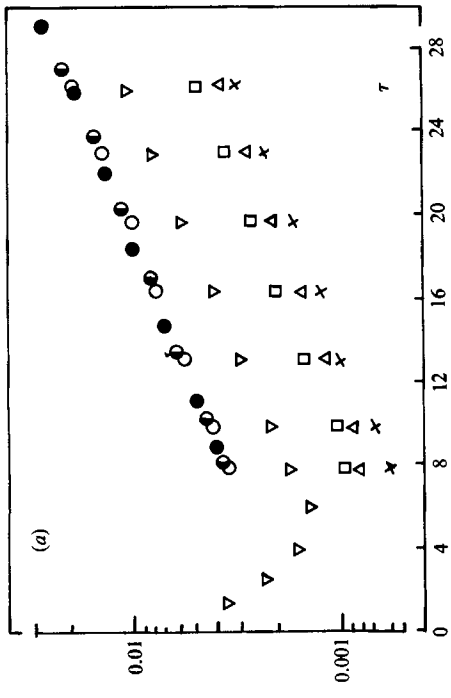

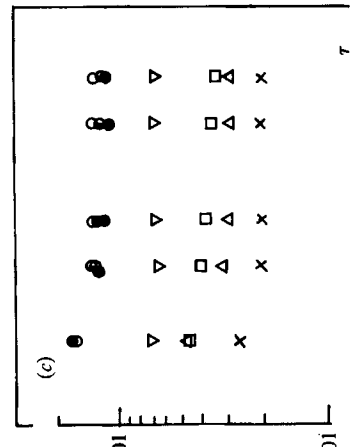

FIGURE 2. Downstream development of the Reynolds stresses and the turbulent kinetic energy. ▽, $\overline{u_1^2}/\bar{U}_c^2$; □, $\overline{u_3^2}/\bar{U}_c^2$; △, $\overline{u_2^2}/\bar{U}_c^2$; ×, $-\overline{u_1 u_2}/\bar{U}_c^2$; ($\bar{U}_c = 13$ m/s in all cases); $\overline{q^2}/\bar{U}_c^2$: ○, $\bar{U}_c = 13$ m/s; ◐, $\bar{U}_c = 9$ m/s; ●, $\bar{U}_c = 6$ m/s. (*a*) Cases A, B, C; (*b*) Cases D, E, F; (*c*) Cases L, M, N; (*d*) Case P (table 1).

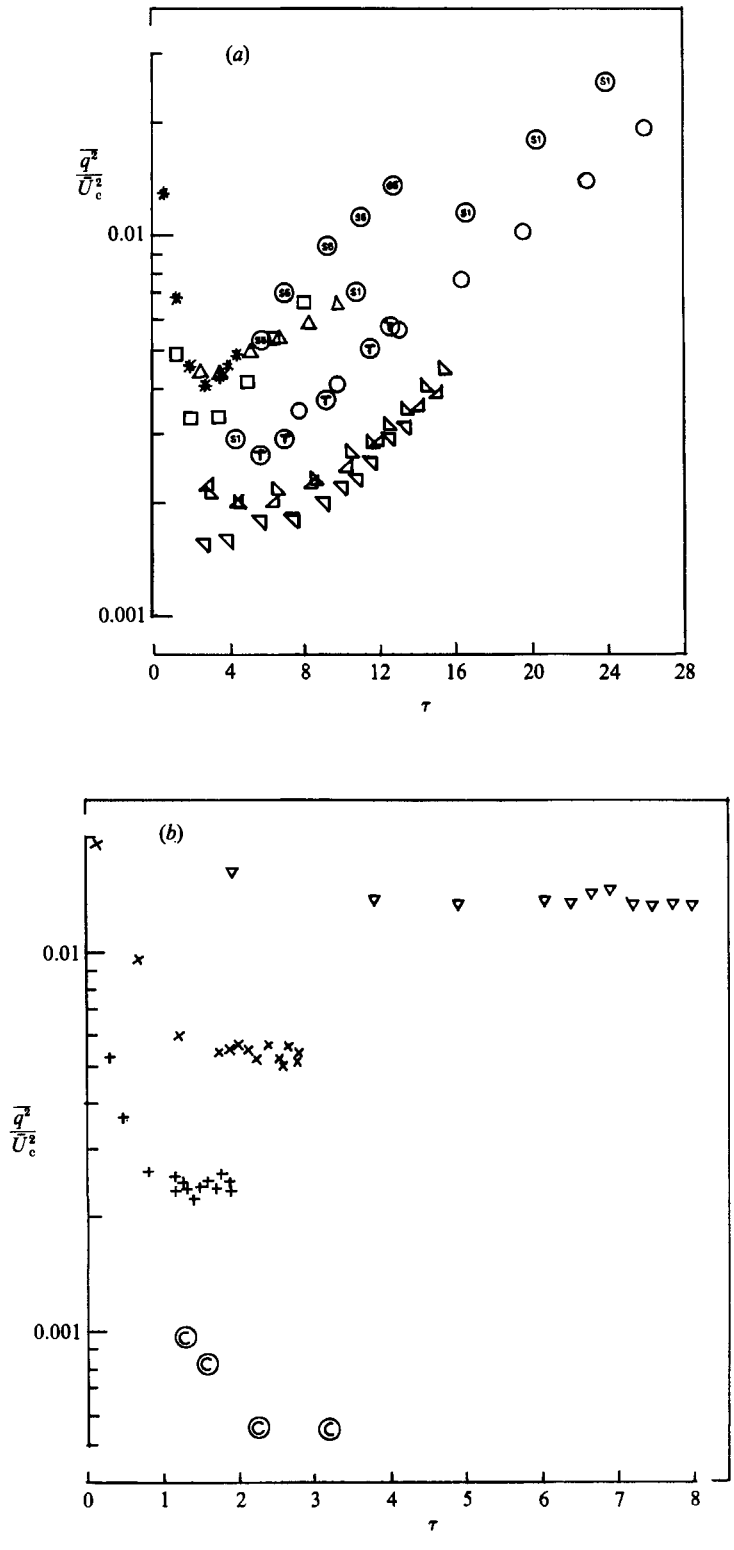

FIGURE 3. Downstream development of the turbulent kinetic energy. Symbols as in table 1.

Case	k_s (m^{-1})	k (m^{-1})	ϵ/P	n_L	k_L (m^{-1})	R_{TM}	U_H (ms^{-1})	τ_e/τ_s	τ_u/τ_s
A	6.56	0.59	0.72	0.81	0.39	16.1	0.0091	3.3	8.4
B	6.56	0.62	0.72	—	—	15.4	0.0081	3.1	8.4
C	7.21	0.66	0.73	—	—	15.1	0.0073	3.4	8.3
D	2.95	0.39	0.61	0.94	0.39	3.9	0.0070	2.2	9.6
E	3.11	0.39	0.63	—	—	4.3	0.0063	2.2	9.3
F	3.05	0.33	0.69	—	—	4.9	0.0055	1.9	8.5
G	3.08	0.23	0.75	0.77	0.36	7.0	0.0071	2.9	9.0
H	3.87	0.36	0.68	0.75	0.30	24.7	0.0076	3.2	9.9
I	3.34	0.33	0.69	0.71	0.30	22.7	0.0073	2.8	9.2
J	3.74	0.36	0.69	0.79	0.30	23.8	0.0075	2.8	9.4
K	1.61	0.13	0.73	—	—	5.9	0.0057	—	6.7
L	2.23	−0.02	1.02	0.94	0.36	8.2	0.0050	2.5	6.5
M	2.23	−0.07	1.09	—	—	8.9	0.0045	2.4	6.5
N	2.23	−0.03	1.04	—	—	10.0	0.0040	2.5	6.5
O	1.05	−0.01	1.04	—	—	4.6	0.0039	—	6.8
P	0.69	0.03	0.87	—	—	3.57	0.0034	—	5.6
CHC	1.05	0	1.0	—	—	9.6	0.0046	2.9	6.1
R1	0.80	0	1.0	—	—	8.3	0.0075	—	—
R2	0.58	0	1.0	—	—	3.2	0.0062	—	—
R3	0.59	0	1.0	—	—	3.5	0.0054	—	—
R4	0.58	0	1.0	—	—	7.3	0.0043	—	—
R5	0.61	0	1.0	—	—	10.7	0.0035	—	—
TC	3.77	0.46	0.57	0.69	0.26	20.3	0.0070	3.7	12.5
S1	6.12	0.55	0.72	0.54	0.31	14.7	0.0027	6.1	8.7
S2	4.75	0.49	0.68	—	—	15.1	0.0025	3.9	9.2
S3	4.89	0.49	0.69	—	—	16.1	0.0027	—	9.1
S4	5.54	0.49	0.72	—	—	11.3	0.0021	—	8.7
S5	4.71	0.58	0.61	0.54	0.31	11.5	0.0020	—	10.2
S6	4.32	0.48	0.65	—	—	20.2	0.0020	—	9.6

TABLE 2. Summary of relevant experimental parameters (conditions as in table 1)

values of k (table 2), it is possible to distinguish two subclasses of flows: those with k close to zero, i.e. flows with roughly constant Reynolds stresses, and those with a clearly positive k, i.e. flows with exponentially growing Reynolds stresses. Exponential growth is relatively weak and, as Rohr *et al.* (1988) point out, it is also compatible with linear growth if an effective origin is used upstream of the physical origin.

The effect of crossing a grid or screen on the turbulence was manifested by a nearly stepwise jump of $\overline{q^2}$ across the obstruction; near the grid, turbulence is produced by the small-scale shear between consecutive jets and wakes of the rods or wires. Grid-generated turbulence decays downstream, so that it seems reasonable to assume that, away from the grids, turbulence production would almost entirely be due to the constant mean shear.

Figure 4 contains the measurements of the dominant components of the dimensionless Reynolds stress tensor

$$K_{ij} = \overline{u_i u_j}/\overline{q^2}. \tag{3}$$

In most cases, the values of K_{ij} in the downstream part of the tunnel were practically constant. Differences between the fully developed values of each K_{ij} for different sets of conditions were relatively small. It is interesting to notice that values of K_{11}, K_{22} and K_{33} near the flow origin were closer to each other than they were away

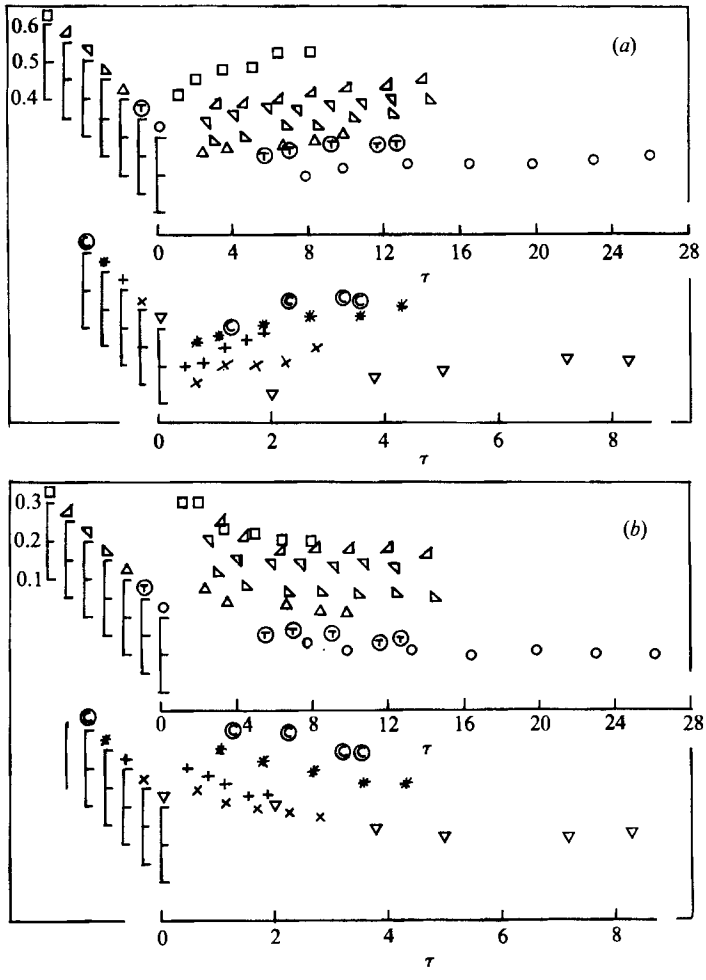

FIGURE 4(*a*, *b*). For caption see facing page.

from it. When the flow crossed a screen, the Reynolds stress tensor was reoriented, tending towards its isotropic form, but, away from the grid, K_{ij} resumed an anisotropic form that is typical for uniformly sheared flows. This form, averaged over all experiments, was

$$K_{ij} = \begin{bmatrix} 0.51 \pm 0.04 & -0.16 \pm 0.01 & 0 \\ -0.16 \pm 0.01 & 0.22 \pm 0.02 & 0 \\ 0 & 0 & 0.27 \pm 0.03 \end{bmatrix}. \tag{4}$$

2.4. *Integral lengthscales*

The streamwise integral lengthscale L_{11} of the streamwise velocity fluctuation was measured by integrating the corresponding autocorrelation coefficient to its first zero and using Taylor's 'frozen flow' approximation. The accuracy of this technique has been demonstrated by Comte-Bellot & Corrsin (1971) and has been found to be satisfactory by Champagne *et al.* (1970) and by Tavoularis & Corrsin (1981*a*) in the case of uniformly sheared flows.

All present and previous measurements of L_{11} have been plotted versus streamwise

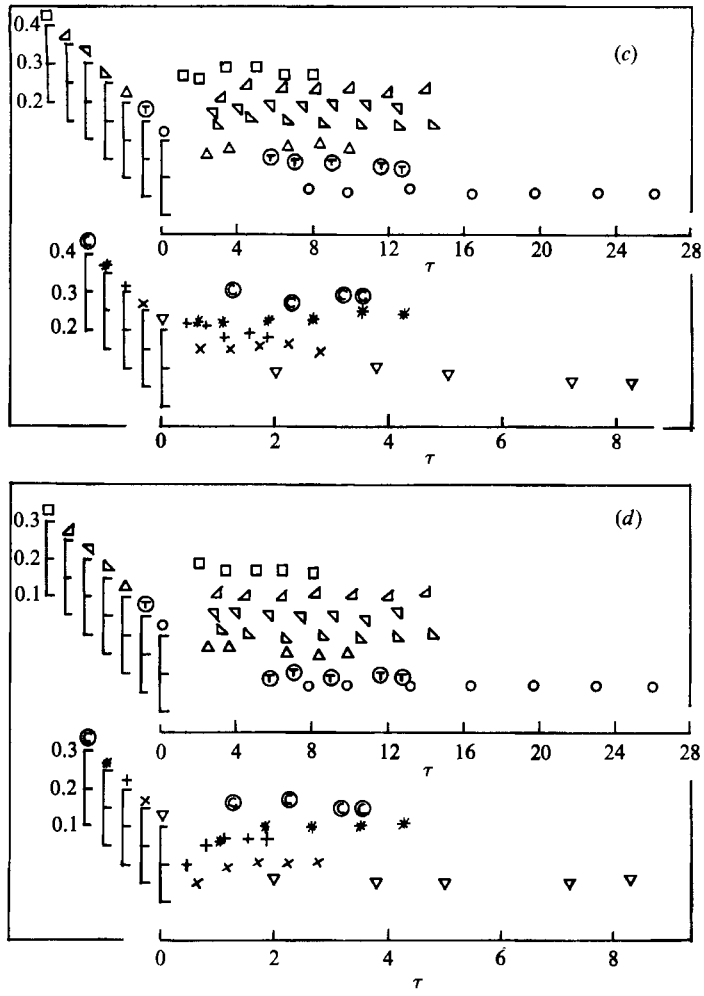

FIGURE 4. Downstream development of the dimensionless Reynolds stresses. Symbols as in table 1. (*a*) K_{11}; (*b*) K_{22}; (*c*) K_{33}; (*d*) $-K_{12}$.

distance in figure 5(*a*) using logarithmic coordinates. Within the experimental uncertainty, one can represent all data using power laws of the type

$$\frac{L_{11}(x_1}{L_r} = \left[\frac{x_1}{x_{rL}}\right]^{n_L}, \tag{5}$$

where L_r and x_{rL} are reference values. The least-squares fitted values of the exponent n_L were on average 0.8 with a standard deviation of about 0.1 (table 2). Considering the relatively large uncertainty in the lengthscales measurement (random experimental error was of the order of 7 %), a linear growth of L_{11} might also be possible as suggested by Harris *et al.* (1977), Tavoularis & Corrsin (1981*a*) and Rohr *et al.* (1988). It is interesting to observe that the growth rate of L_{11} is essentially independent of the shear or any other parameter and that it is substantially higher than the growth rate in nearly isotropic grid turbulence, where integral lengthscales appear to grow according to a power law with an exponent of about 0.4 (see, for instance, Sreenivasan *et al.* 1980). For a given flow generating apparatus, L_{11} was

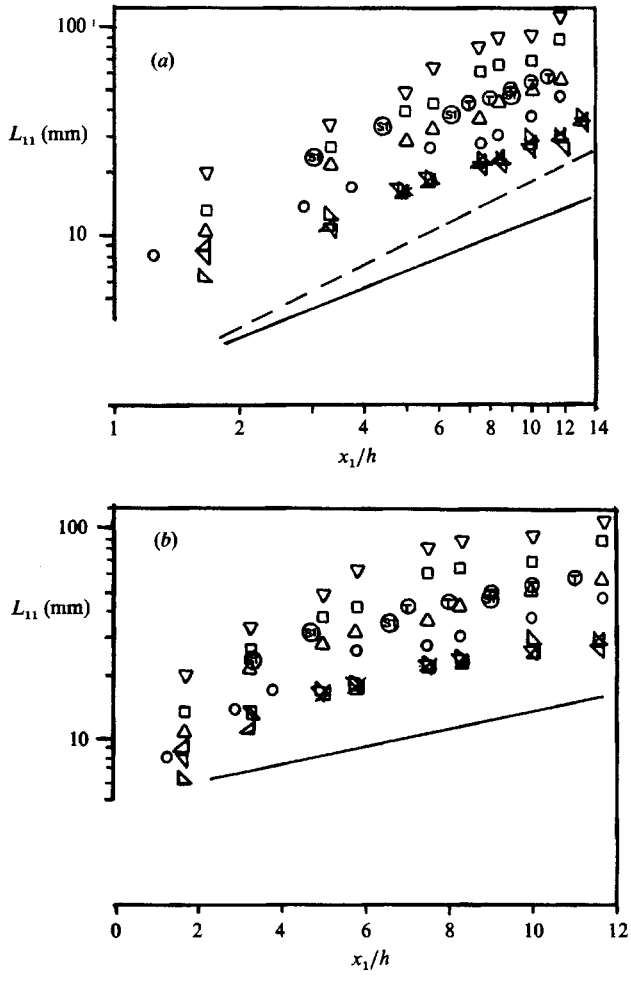

FIGURE 5. Downstream growth of the streamwise integral lengthscale. Symbols as in table 1. (*a*) Logarithmic coordinates: ——, $n_L = 0.8$; – –, $n_L = 1.0$; (*b*) semilogarithmic coordinates: ——, $k_L = 0.33$.

found essentially independent of the wind tunnel speed, which is another indication that the integral lengthscales are not affected by changes of the shear value.

In order to test the possibility of exponential growth, the same scales have been plotted in figure 5(*b*) using semilogarithmic coordinates. An expression of the type

$$\frac{L_{11}}{L_r} = e^{k_L(x_1 - x_r)} \tag{6}$$

may be roughly fitted to the data in the range $5 < x_1/h < 12$, although power laws appear to be more successful in describing the entire range of measurements. The average value of k_L was about 0.33 m^{-1} (table 2).

2.5. *Taylor microscales*

The streamwise Taylor microscale was measured as

$$\lambda_{11} = \left[\frac{\overline{u_1^2}}{\overline{(\partial u_1/\partial x_1)^2}}\right]^{\frac{1}{2}}, \tag{7}$$

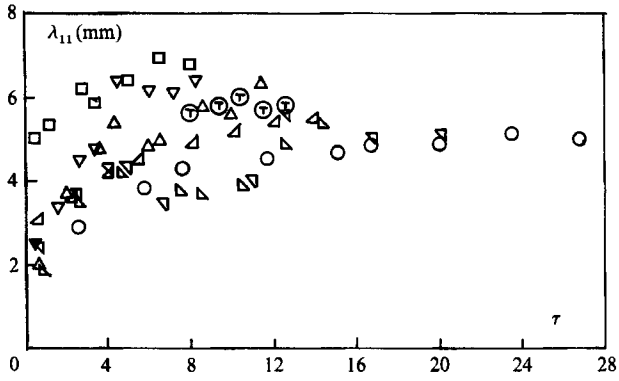

FIGURE 6. Downstream development of the Taylor microscale (λ_{11}). Symbols as in table 1.

where the streamwise derivative was estimated from the time derivative using Taylor's 'frozen flow' approximation. Figure 6 demonstrates that in most cases λ_{11} along the centreline approached constant asymptotes away from the origin. Streamwise constancy of λ_{11} was a central assumption in Tavoularis's (1985) predictions of exponential growth of Reynolds stresses and self-preservation of turbulence structure. It also implies that the relative magnitudes of production and dissipation should remain unchanged.

3. Analysis and discussion of results

3.1. *Definition of scaling parameters*

In an unbounded uniformly sheared flow, the sole externally imposed parameter is the value of the mean shear, which represents both the mean vorticity and the mean strain rate. This value imposes the characteristic 'straining' time

$$\tau_s = (\mathrm{d}\overline{U_1}/\mathrm{d}x_2)^{-1}. \tag{8}$$

In the hypothetical case of unbounded, transversely homogeneous shear flow there is neither an external lengthscale nor a velocity scale and further non-dimensionalization becomes impossible, unless one assigns an arbitrary value to one of these parameters. In laboratory generated flows, it has been demonstrated (see also Rohr *et al.* 1988), that the centreline velocity is an appropriate scale for non-dimensionalizing the Reynolds stresses. Then it is possible to define a flow generator constant, k_s, as

$$k_s = \frac{1}{\bar{U}_c}\frac{\mathrm{d}\bar{U}_1}{\mathrm{d}x_2}, \tag{9}$$

which has dimensions of inverse length. One might anticipate that the value of k_s could have a qualitative effect on the turbulence structure. The dimensionless total strain imposed upon the turbulence at a particular distance from the origin is simply

$$\tau = k_s x_1 \tag{10}$$

For each particular value of k_s, a self-preserving structure must be independent of τ.

The average size of the energy-containing turbulent eddies can be represented by integral lengthscales, most conveniently the streamwise one, L_{11}. Such scales generally grow downstream from an initial value, which is set by the spacing of the

flow generating elements. In the absence of grids and screens, this spacing is clearly the width of the individual channels of the shear generator and flow separator. When one or more grids or screens are inserted, the initial scale appears to be a complicated function of upstream flow characteristics, grid mesh size and solidity. In a crude way one might infer from the present results that the initial lengthscale is comparable with the larger of either the flow separator channel width or grid mesh size. A corresponding timescale, which can be interpreted as the 'turnover time' of a typical turbulent eddy (Compte-Bellot & Corrsin 1971), is

$$\tau_e = L_{11}/u_1'. \tag{11}$$

Another timescale that is commonly used in turbulence modelling is the typical 'lifetime' of the energy-containing eddies

$$\tau_u = \overline{q^2}/\epsilon, \tag{12}$$

where ϵ is the turbulent kinetic energy dissipation rate. If one further defines a characteristic time for transport of $\overline{q^2}$ by the mean flow as

$$\tau_T = (k\overline{U_c})^{-1}, \tag{13}$$

where k is the exponent in the stress growth law, is is possible, with the use of the simplified kinetic energy equation (Tavoularis 1985), to derive a relation between the two latter timescales and τ_s as

$$\frac{1}{\tau_u} = \frac{-K_{12}}{\tau_s} - \frac{1}{2\tau_T}. \tag{14}$$

3.2. *Tests of self-preservation*

'The hypothesis of self-preserving development of a turbulent flow assumes that all aspects of the motion except those directly influenced by viscosity have similar forms at all stages, the differences being described wholly by changes of velocity and lengthscales which are functions of time (in decaying turbulence) or of the position in the flow direction' (Townsend 1976, pp. 60–61). The mean velocity field, $\bar{U}_1(x_2)$, obviously meets the criteria of self-preservation, since it is essentially invariant within the wind tunnel. Second-order turbulent moments are also self-preserving in the bulk of the flow, since their relative magnitudes remain constant, as demonstrated by the constancy of all components of K_{ij}. This was true for all cases, both those with constant and those with growing stresses. Integral lengthscales appear to follow a growth pattern, which could be different from that of the kinetic energy. Also, relative magnitudes of integral scales in different directions appear to be roughly constant for both 'low-shear' (Champagne *et al.* 1970) and 'high-shear' Tavoularis & Corrsin 1981*a*) cases.

In conclusion, all existing evidence supports the hypothesis that uniformly sheared turbulence in wind tunnels achieves an approximately self-preserving state in which turbulent velocity and lengthscales follow well-defined laws of downstream evolution and properly non-dimensionalized quantities remain invariant.

3.3 *Criteria for the evolution of turbulent kinetic energy*

As discussed earlier, it has been possible to identify two subclasses of uniformly sheared turbulent flows, namely flows with growing stresses and flows with roughly constant stresses. One might then speculate on the existence of a third subclass of flows with decaying stresses, which has actually been predicted theoretically for

'extremely weak' turbulence (e.g. by Deissler 1961, 1965). The experimental confirmation of the third subclass is inconclusive. The few cases in Rose's (1970) experiments that he interprets as decaying sheared turbulence are subject to an extremely low signal-to-noise ratio; they are also contradicted by his figure 6. Our experiments have not yielded any case having a negative value of k that deviated from zero by an amount larger than the measuring uncertainty. The limiting case $\mathrm{d}\bar{U}_1/\mathrm{d}x_2 = 0$ can, of course, be represented by grid-generated, unsheared turbulence, whose second moments decay. However, the unsheared case is a singular limit since it does not satisfy the assumption $\epsilon/\overline{q^2} = \text{constant}$, which was the basis for the derivation of an exponential law.

We now proceed to identify parameters that possibly affect the balance between production and dissipation and thus the evolution law of the turbulent stresses and the turbulent kinetic energy. The mean shear is certainly a relevant parameter, because, all other external conditions being the same, an increase of mean shear leads from a constant-$\overline{q^2}$ flow (Champagne *et al.* 1970) to a growing-$\overline{q^2}$ flow (Harris *et al.* 1977; Tavoularis & Corrsin 1981*a*). However, the value of $\mathrm{d}\bar{U}_1/\mathrm{d}x_2$ alone is not sufficient to determine the energy growth law; this can be seen by comparing cases with about the same shear but different centreline velocities, for examples cases M and K versus case F and case L versus case E in table 1.

Harris *et al.* (1977) have suggested that it is the value of the total strain τ that determines whether a state of growing stresses has been achieved and that, if 'low-shear' flows were permitted to achieve a sufficiently large τ by extending the wind tunnel length, they would also exhibit growing stresses. Rohr *et al.* (1988) further suggest a 'threshold' of $\tau \approx 4$ above which turbulence grows. Some of the present measurements contradict these hypotheses. As figure 3 demonstrates, the kinetic energy in case L was practically constant in the range $4 < \tau < 8$. Although this case has the largest lengthscales and, presumably, the strongest wind-tunnel wall interference, it seems unlikely that suppression of kinetic energy growth can be solely attributed to that effect. It should also be remembered that case L has a self-preserving Reynolds stress tensor and integral lengthscales which continue growing at a constant rate.

Following Tavoularis (1985), the kinetic energy exponent coefficient can be expressed as

$$k = -2K_{12}(1-\epsilon/P)\,k_{\mathrm{s}}, \tag{15}$$

where the kinetic energy production is

$$P = -\overline{u_1 u_2}\frac{\mathrm{d}\bar{U}_1}{\mathrm{d}x_2}. \tag{16}$$

The values of the ratio ϵ/P, computed from measurements of k and K_{12} using (14), are plotted in figure 7(*a*) versus k_{s}. Based on the value of ϵ/P, it is possible to identify two subclasses of flows, as

$$\text{'low-shear'}: \quad \epsilon/P \approx 1,$$

$$\text{'high-shear'}: \quad \epsilon/P < 1.$$

The scatter of ϵ/P in the second subclass about the average value 0.68 ± 0.06 seems to be non-systematic. Using the average values $\epsilon/P = 0.68$ and $K_{12} = -0.16$, one can derive the relation

$$k \approx 0.1 k_{\mathrm{s}} \tag{17}$$

which, as shown in figure 7(*b*), is compatible with all available measurements at sufficiently large k_{s}. It is therefore concluded that the asymptotic growth rate of $\overline{q^2}$

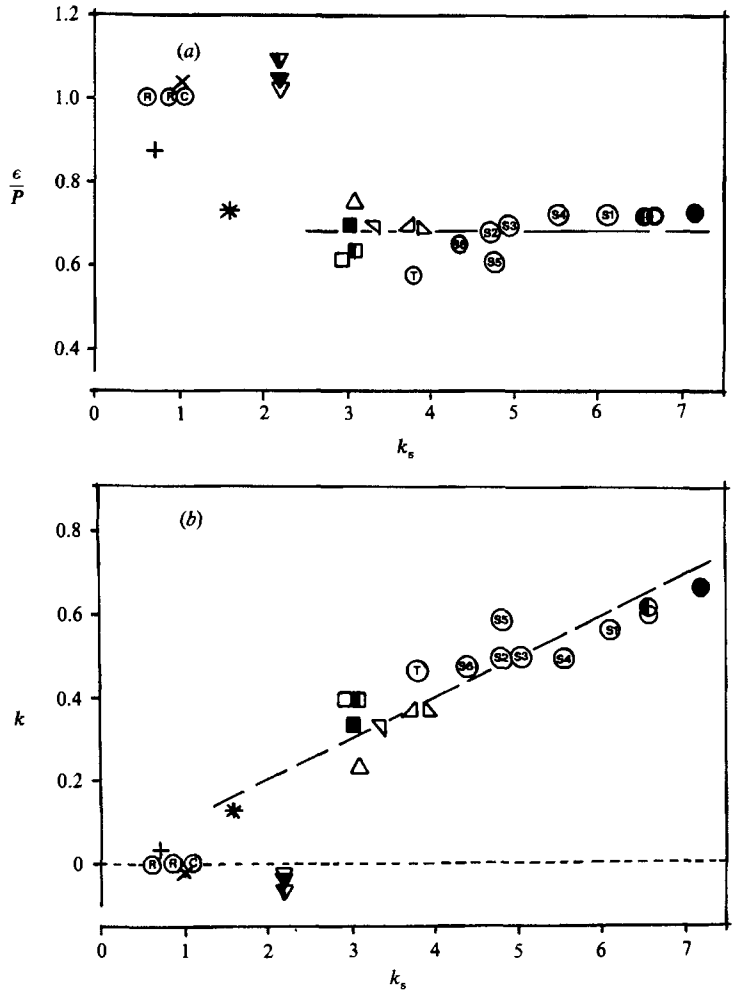

FIGURE 7. (*a*) The ratio ϵ/P and (*b*) the exponent coefficient k, versus k_s. Symbols as in table 1.

in wind-tunnel-confined, uniformly sheared turbulence depends on the flow generator constant k_s. For small k_s, $\overline{q^2}$ may maintain a constant value, while for large k_s it grows exponentially; in the latter case the exponent is proportional to k_s, although the ratio ϵ/P is independent of k_s. Independent estimates of the ratio ϵ/P, based on the measured Taylor microscale, are compatible with the existence of two distinct subclasses.

The present experiments cover a range of k_s that is substantially wider than those in previous ones. Although, in our opinion, the large-k_s range has been adequately described by (2) and (17), it would have been desirable to further scrutinize the low-k_s range. Unfortunately, our attempts to decrease k_s by using high-solidity screens led to inhomogeneous flows. It is also clear that the uncertainty in the determination of k and ϵ/P increases dramatically as k_s decreases.

In addition to the above, we have considered several other possible criteria for the evolution of kinetic energy, such as the quantities

$$\frac{M(\text{or } M_g)}{\bar{U}_c}\frac{d\bar{U}_1}{dx_2}, \quad \frac{L_{11}}{\bar{U}_c}\frac{d\bar{U}_1}{dx_2}, \quad \frac{L_{11}}{u_1'}\frac{d\bar{U}_1}{dx_2}.$$

None of the tested criteria were successful in separating the two subclasses of flows identified above.

3.4. *On Hasen's stability theory*

In her nonlinear stability analysis of uniformly sheared flows, Hasen (1967) concluded that two-dimensional disturbances would decay if their amplitude were smaller than a 'barrier' velocity and that they would not decay otherwise. She also found that the barrier velocity was bounded from above and below by two quantities, which were proportional to the velocity

$$U_{\mathrm{H}} = \frac{l_{\mathrm{H}}\, \mathrm{d}\overline{U_1}/\mathrm{d}x_2}{R_{\mathrm{H}}^{\frac{2}{3}}}, \tag{18}$$

where l_{H} is the characteristic length of the disturbances and the Reynolds number was defined as

$$R_{\mathrm{H}} = \frac{\mathrm{d}\overline{U_1}/\mathrm{d}x_2\, l_{\mathrm{H}}^2}{\nu}. \tag{19}$$

Substituting (19) into (18), one gets

$$U_{\mathrm{H}} = \left[\frac{1}{l_{\mathrm{H}}}\frac{\mathrm{d}\overline{U}_1}{\mathrm{d}x_2}\right]^{\frac{1}{3}} \nu^{\frac{2}{3}}. \tag{20}$$

According to this theory, no finite-amplitude, two-dimensional disturbances would decay if $U_{\mathrm{H}} \to 0$, which can occur either when $\mathrm{d}\overline{U_1}/\mathrm{d}x_2 = 0$ or when $l_{\mathrm{H}} \to \infty$. Consequently, one might speculate that the lower U_{H} for a flow is, the 'more unstable' the flow would be. This appears to contradict the intuitive expectation that, for given l_{H} and ν, a flow should become 'more stable' as $\mathrm{d}\overline{U_1}/\mathrm{d}x_2$ decreases. On the other hand, the implication of increased stability as l_{H} grows is compatible with intuition. Rose's (1970) attempt to correlate his results with Hasen's theory is not conclusive in our opinion, first because, as indicated earlier, his few cases of alleged decaying turbulence are questionable, and second because his study addresses only the effect of lengthscale and does not take into account the amplitude of disturbances. In grid turbulence, amplitudes and scales are inherently coupled, as demonstrated by the fact that the energy decay law is a function of grid mesh size. A proper test of Hasen's theory should involve a laminar shear flow and disturbances with independently controlled amplitudes and wavelengths. In any case, calculations of U_{H} based on maximum apparatus spacing (table 2) show that, in general, large values of U_{H} correspond to growing (unstable?) turbulence, in contrast to implications of Hasen's theory. In view of this discussion, the apparent success of using U_{H} as a criterion for the evolution of $\overline{q^2}$ (Karnik & Tavoularis 1983) might be coincidental. The present discussion is consistent with that of Rohr *et al.* (1988).

3.5. *Scaling of the turbulent stresses*

A general feature of self-preserving turbulent shear flows such as two- and three-dimensional wakes, jets, plumes etc. is that the 'effective Reynolds number'

$$R_{\mathrm{T}} = \frac{\Delta U l}{\nu_{\mathrm{T}}} \tag{21}$$

(ΔU is a characteristic mean velocity difference, l is a transverse length characteristic of the mean flow extent and $\nu_{\mathrm{T}} = -\overline{u_1 u_2}/(\partial\overline{U_1}/\partial x_2)$ is the 'eddy viscosity') shows small variation within each class of flows and has values comparable with the lower critical Reynolds number for laminar instability (Corrsin 1957). The applicability of

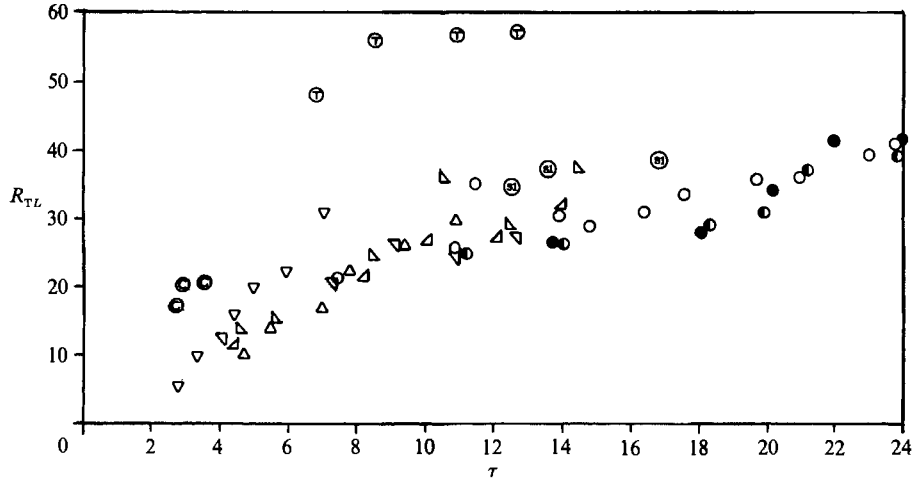

FIGURE 8. Variation of the 'effective Reynolds number' based on L_{11}. Symbols as in table 1.

such a postulate to uniformly sheared flows is quite plausible, in view of their reasonable transverse homogeneity.

The parameters ΔU and l are, most likely, related to the imposed timscale τ_s as

$$\frac{\Delta U}{l} = \frac{\mathrm{d}\overline{U_1}}{\mathrm{d}x_2} = \tau_s^{-1}, \tag{22}$$

which leads to the following expression for R_T:

$$R_T = \frac{(\mathrm{d}\overline{U_1}/\mathrm{d}x_2)^2 l^2}{-K_{12}\overline{q^2}}, \tag{23}$$

containing l as the sole unspecified quantity. A lengthscale that might be appropriate as l is the integral lengthscale, L_{11}. Figure 8 shows that the corresponding Reynolds number, R_{TL}, generally increases with increasing total strain for small values of τ. In regions where as exponential kinetic energy growth has been established, R_{TL} presents a very small variation, reflecting the fact that the growth rates of stresses and L_{11} in such cases are not very different. A proposition that is equivalent to the universality of R_{TL} has been made by Harris *et al.* (1977). We note, however, that their figure 5 appears to contain a numerical error reducing the difference between 'low-shear' and 'high-shear' results. All present measurements at large τ have R_{TL} values in the range 30–40, which is also the case for some of Rohr *et al.*'s (1988) results. The asymptotic value for the Tavoularis & Corrsin (1981*a*) experiments was about 57.

L_{11} is not an externally imposed scale; however, as mentioned earlier, its starting value is related to the spacing of the flow generator. When measurements of L_{11} are not available, it would be useful to define R_T based on a clearly defined external length. Among other choices, it seems that variation of R_T is reduced if the maximum among the spacings between the elements in the shear generator and/or grids or screens is used as l. The so computed R_{TM} (table 2) presents a variation between 3.2 and 10.7 for the constant-stress cases, which is quite small, considering that the stresses themselves range over four orders of magnitude. In the cases with growing stresses, R_{TM} decreases monotonically downstream but its variation among different cases is also relatively small.

A related quantity, the ratio of eddy turnover time over the straining time,

$$\frac{\tau_e}{\tau_s} = \frac{L_{11}}{u_1'}\frac{d\bar{U}_1}{dx_2}, \tag{24}$$

also has a relatively narrow range (table 2), taking values between 1.9 and 3.7. The ratio of eddy lifetime over the straining time

$$\frac{\tau_u}{\tau_s} = \frac{1}{(\epsilon/P)(-K_{12})} \tag{25}$$

has nearly constant asymptotic values, which are about 6.5 for the 'low-shear' and 9.0 for the 'high-shear' flows.

3.6. *An 'exact' expression for the pressure–strain rate covariance tensor*

For transversely homogeneous flows with uniform mean shear, the balance equation for the Reynolds stress tensor is simplified to

$$\overline{U_1}\frac{d\overline{u_i u_j}}{dx_1} = -\overline{u_2 u_j}\frac{d\bar{U}_1}{dx_2}\delta_{i1} - \overline{u_2 u_i}\frac{d\bar{U}_1}{dx_2}\delta_{j1} + \frac{1}{\rho}\overline{p\left[\frac{\partial u_i}{\partial x_j}+\frac{\partial u_j}{\partial x_i}\right]} - 2\nu\overline{\frac{\partial u_i}{\partial x_k}\frac{\partial u_j}{\partial x_k}} \tag{26}$$

which, in condensed form, becomes

$$T_{ij} = P_{ij} + \phi_{ij} - 2\epsilon_{ij}. \tag{27}$$

The mean convection term, T_{ij}, can be computed exactly for the two subclasses of flows with either constant or exponentially growing stresses as

$$T_{ij} = 2\left(1-\frac{\epsilon}{P}\right)PK_{ij}. \tag{28}$$

This form of T_{ij} happens to be identical to the one deduced from Rodi's (1976) algebraic stress model. The 'production' tensor can be written as

$$P_{ij} = \left[\frac{K_{2j}}{K_{12}}\delta_{i1} + \frac{K_{2i}}{K_{12}}\delta_{j1}\right]P, \tag{29}$$

and has only two independent non-zero components, P_{11} and P_{12}.

After rearranging the various terms and without any further assumption or approximation, the pressure–strain rate covariance, made dimensionless with the production P, takes the following form for the present class of flows:

$$\frac{\phi_{ij}}{P} = -\left[\frac{P_{ij}}{P} - \tfrac{2}{3}\delta_{ij} - 2m_{ij}\right] - 2(m_{ij}-d_{ij})\frac{\epsilon}{P}, \tag{30}$$

where the anisotropy tensors of Reynolds stresses and dissipation rate are defined as

$$m_{ij} = K_{ij} - \tfrac{1}{3}\delta_{ij}, \tag{31}$$

$$d_{ij} = \frac{\epsilon_{ij}}{\epsilon} - \tfrac{1}{3}\delta_{ij}. \tag{32}$$

3.7. *On the anisotropy of the turbulent stresses and the dissipation rate*

Figure 9 summarizes the measurements of anisotropy of the Reynolds stress tensor, plotted versus the flow generator constant k_s. The data contain significant scatter, which could be partly attributed to imperfections in the apparatus and, to a lesser

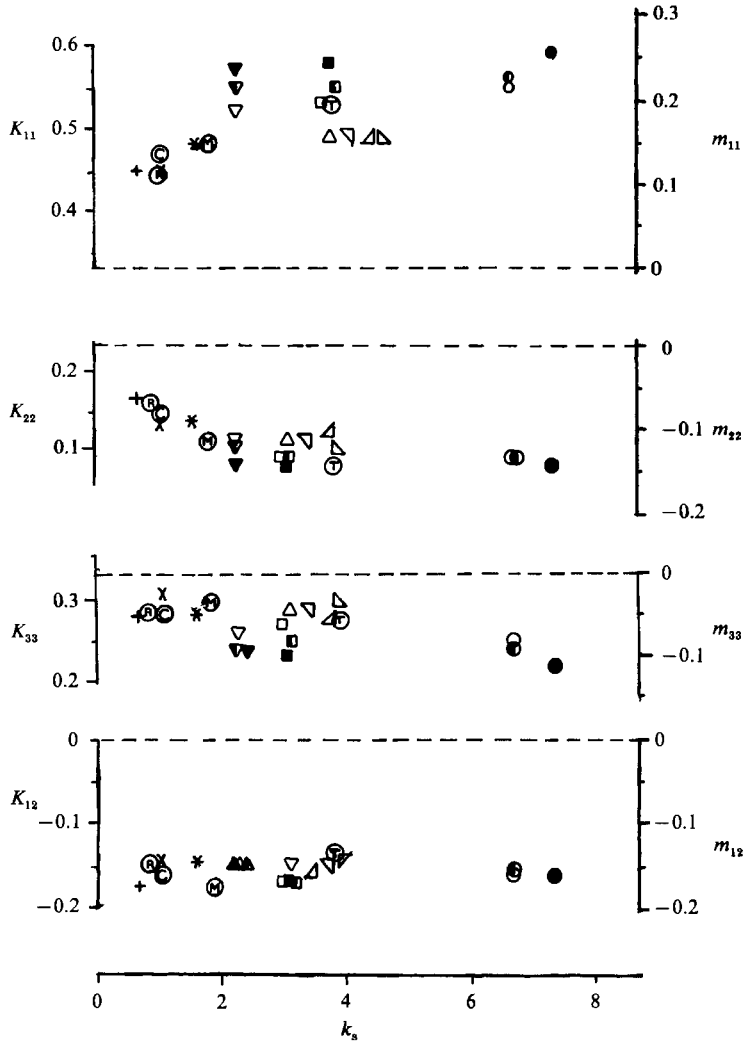

FIGURE 9. Dependence of the Reynolds stress tensor anisotropy on the flow generator constant, k_s. Symbols as in table 1.

extent, to measurement inaccuracies. However, it is evident that 'low-shear' cases ($k_s < 2$) have somewhat lower anisotropies of the diagonal components of K_{ij} than 'high-shear' cases have and that, for $k_s > 2$, m_{ij} is practically constant. The cross-anisotropy m_{12} does not appear to vary at all with k_s.

The anisotropy of the dissipation rate tensor is hard to measure or even estimate accurately, although previous investigators agree that ϵ_{ij} is non-isotropic. Weinstock & Burk (1985) have integrated spectra measured by Champagne *et al.* (1970) to derive the values

$$\frac{\epsilon_{11}}{\epsilon} = 0.36, \quad \frac{\epsilon_{22}}{\rho} = 0.30, \quad \frac{\epsilon_{33}}{\epsilon} = 0.34.$$

The only available measurements of velocity derivates (Tavoularis & Corrsin 1981*b*) in a high-shear flow indicate a much stronger streamwise anisotropy, as

$$\frac{\epsilon_{11}}{\epsilon} = 0.6,$$

and the spectra measured by Tavoularis & Corrsin (1981*a*), show that ϵ_{22} and ϵ_{33} may not vary significantly from each other, which implies that

$$\frac{\epsilon_{22}}{\epsilon} \approx \frac{\epsilon_{33}}{\epsilon} \approx 0.2.$$

It is interesting to note that in a large-scale simulation of uniformly sheared turbulence, Feiereisen *et al.* (1982) found that d_{ij} is roughly proportional to m_{ij} with coefficient 0.85 for all stresses when the turbulent Reynolds number was in the range between 15 and 120. This leads to the relation

$$\frac{\epsilon_{ij}}{\epsilon} \approx 0.85K_{ij} + 0.05\delta_{ij}, \tag{33}$$

with the typical values

$$\frac{\epsilon_{11}}{\epsilon} \approx 0.48, \quad \frac{\epsilon_{22}}{\epsilon} \approx 0.24, \quad \frac{\epsilon_{33}}{\epsilon} \approx 0.28, \quad \frac{\epsilon_{12}}{\epsilon} \approx -0.14.$$

3.8. *Comments on some turbulence models*

Among the most successful and popular turbulence models are the various 'second-order' closure schemes. Drawing an analogy with the constitutive laws of materials in continuum mechanics, these models attempt to express the physical properties of turbulence in a universal mathematical form (for a comprehensive discussion, see Lumley 1978). All models contain a number of adjustable numerical coefficients, which are usually evaluated from measurements in flows with simple geometry, such as nearly isotropic turbulence and uniformly sheared turbulence. The application of a general model to a 'simple' flow and the subsequent generalization of the results require a great deal of caution. As an illustration of some inconsistencies that may arise from the indiscriminate use of measurements such as the present ones in model constant evaluation, we shall present the following discussion, which focuses upon the pressure–strain rate correlation, ϕ_{ij}. This tensor has been the object of modelling, since, in general, it cannot be measured or evaluated theoretically in terms of other parameters. Following Rotta's (1951) analysis, ϕ_{ij} is customarily decomposed into two parts

$$\phi_{ij} = \phi_{ij,1} + \phi_{ij,2}, \tag{34}$$

which represent, respectively, effects of fluctuations and of mean strain rate and are modelled separately. A number of frequently used models (Rotta 1951; Naot, Shavit & Wolfshtein 1973; Launder, Reece & Rodi 1975) can be represented by a general form, which, when applied to uniformly sheared flows, becomes

$$\frac{\phi_{ij}}{P} = -C_{ij,2}\left[\frac{P_{ij}}{P} - \tfrac{2}{3}\delta_{ij}\right] - 2C_{ij,1}\, m_{ij}\frac{\epsilon}{P}, \tag{35}$$

where repeated indices are not summed. Comparing the 'exact' equation (30) and the modelled equation (35), one may observe that they both contain two terms, one proportional to ϵ/P and another which may depend on ϵ/P only implicitly through m_{ij} and $C_{ij,2}$ respectively. Since dependence of m_{ij} on ϵ/P is rather weak for uniformly sheared flows, at least for large values of k_s, one may consider the possibility that the corresponding two terms of (30) and (35) match separately, which implies that

$$C_{ij,1} = 1 - \frac{d_{ij}}{m_{ij}}, \tag{36}$$

$$C_{ij,2} = 1 - \frac{2m_{ij}}{(P_{ij}/P) - \frac{2}{3}\delta_{ij}}. \tag{37}$$

As it is generally accepted that the dissipation anisotropy vanishes at large Reynolds numbers, one might further speculate that

$$C_{ij,1} \to 1 \quad \text{as} \quad R_\lambda \to \infty,$$

in which case the relevant components of $C_{ij,2}$ would simply be

$$C_{11,2} = \tfrac{3}{2}(1-K_{11}), \quad C_{22,2} = 3K_{22}, \tag{38a, b}$$

$$C_{33,2} = 3K_{33}, \quad C_{12,2} = 1-2\frac{K_{12}^2}{K_{22}}. \tag{38c, d}$$

It is then obvious that the tensor $C_{ij,2}$ can be reduced to a scalar only when

$$K_{22} = K_{33}, \quad K_{12} = [\tfrac{1}{2}K_{22}(K_{11}-K_{22})]^{\frac{1}{2}}. \tag{39a, b}$$

Instead of requiring satisfaction of conditions (39), one may approximate $C_{ij,2}$ by a scalar obtained by averaging (38), i.e.

$$\overline{C_2} = \frac{1}{4}\left(1+4.5(K_{22}+K_{33})-2\frac{K_{12}^2}{K_{22}}\right). \tag{40}$$

The previous approach was based upon the assumption that K_{ij} was independent of ϵ/P. In general, however, modellers have not employed this assumption but computed values of $C_{ij,1}$ and $C_{ij,2}$ that satisfy particular experimental conditions. This approach will reproduce the proper values of m_{ij}, provided that a sufficient number of constants are adjusted to the measurements of K_{ij}. If, for example, one computes the eight independent components of $C_{ij,1}$ and $C_{ij,2}$ by using the values of K_{ij} in the experiments of Champagne *et al.* (1970) and Harris *et al.* (1977) and uses these values to 'postdict' K_{ij}, the 'postdiction' of K_{ij} in these two cases will be perfect. More sophisticated evaluations of constants have included the effect of dissipation anisotropy (Weinstock & Burk 1985) through spectral estimates based on measurements.

Nevertheless, considering (30), one is tempted to observe that any need for constant evaluation would be eliminated if one assumed forms for $\phi_{ij,1}$ and $\phi_{ij,2}$ that in large-R_λ, homogeneous, uniformly sheared flow reduce to

$$\phi_{ij,1} = -2(K_{ij}-\tfrac{1}{3}\delta_{ij})\,\epsilon, \tag{41}$$

$$\phi_{ij,2} = -\left[\frac{P_{ij}}{P}-2K_{ij}\right]P. \tag{42}$$

It might also be illuminating to point out that if, for a moment, one assumes that $d_{ij} \approx m_{ij}$, equation (30) takes the extremely simple form

$$\frac{\phi_{ij}}{P} = -\left[\frac{P_{ij}}{P}-2K_{ij}\right], \tag{43}$$

which, although not of general applicability to inhomogeneous turbulence, may well approximate results in uniformly sheared flows.

We shall close this discussion by presenting values of K_{ij} computed by equating (30) and (35) and assigning values to the model constants. For simplicity, we have only considered the case of isotropic ϵ_{ij}. In table 3, cases I*a* ('low-shear', $\epsilon/P \approx 1.0$) and I*b* ('high-shear', $\epsilon/P \approx 0.68$) correspond to the commonly used scalar values $C_{ij,1} = 1.8$ and $C_{ij,2} = 0.6$. Cases II*a* and II*b* are independent of the ratio ϵ/P and correspond to the value of $C_{ij,1} = 1.0$ and the 'custom fitted' $C_{ij,2}$ through (38) (case

Case	ϵ/P	C_1	$C_{11,2}$	$C_{22,2}$	$C_{12,2}$	$C_{33,2}$	K_{11}	K_{22}	K_{33}	$-K_{12}$
Ia	1.0	1.8	0.60	0.60	0.60	0.60	0.48	0.26	0.26	0.17
Ib	0.68	1.8	0.60	0.60	0.60	0.60	0.51	0.245	0.245	0.18
IIa	Any	1.0	0.73	0.66	0.81	0.77	0.51	0.22	0.27	0.16
IIb	Any	1.0	0.74	0.74	0.74	0.74	0.51	0.245	0.245	0.18

TABLE 3. 'Postdicted' values of Reynolds stresses

IIa) or the average $\overline{C_2}$ through (40) (case IIb). All of the above combinations of constants, and possibly many others, demonstrate reasonable agreement with measurements, although it is evident that the anisotropy of K_{ij} can be only 'posdicted' if a tensorial form of the constants is employed.

Financial support for this project was provided by the Natural Sciences and Engineering Research Council of Canada. We thank the referees and G. Holloway for useful comments on the manuscript.

REFERENCES

BURGERS, J. M. & MITCHNER, M. 1953 On homogeneous non-isotropic turbulence connected with a mean motion having a constant velocity gradient. *Konik. Ned. Akad. v. Wet.* B **15**, 228; part II, 383.

CAMBON, C., JEANDEL, D. & MATHIEU, J. 1981 Spectral modelling of homogeneous non-isotropic turbulence. *J. Fluid Mech.* **104**, 247.

CHAMPAGNE, F. H., HARRIS, V. G. & CORRSIN, S. 1970 Experiments on nearly homogeneous shear flow. *J. Fluid Mech.* **41**, 81.

COMTE-BELLOT, G. & CORRSIN, S. 1971 Simple Eulerian time correlation of full- and narrow-band velocity signals in grid generated, "isotropic" turbulence. *J. Fluid Mech.* **48**, 273.

CORRSIN, S. 1957 Some current problems in turbulent shear flows. *Proc. 1st Naval Hydr. Symp. Nat. Acad. Sci./Nat. Rec. Counc., Washington DC*, publ. 515.

CORRSIN, S. & KOLLMAN, W. 1977 Preliminary report on sheared cellular motion as a qualitative model of homogeneous turbulent shear flow. *Turbulence in Internal Flows, Project SQUID Workshop* (ed. S. N. B. Murthy). Hemisphere.

COURSEAU, P. A. & LOISEAU, M. 1978 Contribution à l'analyse de la turbulence homogène anisotrope. *J. Méc.* **17**, 245.

CRAYA, A. 1958 Contribution à l'analyse de la turbulence associée à des vitesses moyennes. *Publ. Scien. et Techn. du Ministere de l'Air* 345.

DEISSLER, R. G. 1961 Effects of inhomogeneity and of shear flow in weak turbulent fields. *Phys. Fluids* **4**, 1187.

DEISSLER, R. G. 1965 Problem of steady state shear flow turbulence. *Phys. Fluids* **8**, 391.

DEISSLER, R. G. 1970 Effect of initial condition on weak homogeneous turbulence with uniform shear. *Phys. Fluids* **13**, 1868.

FEIEREISEN, W. J., SHIRANI, E., FERZIGER, J. H. & REYNOLDS, W. C. 1982 Direct simulation of homogeneous turbulent shear flow on Illiac IV computer: Applications to compressible and incompressible modelling. In *Turbulent Shear Flows*, vol. 3 (ed. L. J. S. Bradbury, F. Durst, B. E. Launder, F. W. Schmidt & J. H. Whitelaw), p. 309. Springer.

FOX, J. 1964 Velocity correlations in weak turbulent shear flow. *Phys. Fluids* **7**, 562.

GENCE, J. N., ANGEL, Y. & MATHIEU, J. 1978 Partie linéaire des corrélations metant en jeu la pression dans une turbulence à un cisaillement et un effeect de gravité. *J. Méc.* **17**, 329.

HARRIS, V. G., GRAHAM, J. A. & CORRSIN, S. 1977 Further experiments in nearly homogeneous turbulent shear flow. *J. Fluid Mech.* **81**, 657.

HASEN, E. M. 1967 A non-linear theory of turbulence onset in a shear flow. *J. Fluid Mech.* **29**, 721.

HWANG, W. S. 1971 Experimental investigation of turbulent shear flows. Ph.D. dissertation, University of Virginia.

KARNIK, U. M. 1983 Experiments on uniformly sheared turbulence. M.A.Sc. thesis, University of Ottawa.

KARNIK, U. & TAVOULARIS, S. 1983 The asymptotic development of nearly homogeneous turbulent shear flow. Proc. 4th Symp. Turb. Shear Flows, Karlsruhe, p. 14.18.

KARNIK, U. & TAVOULARIS, S. 1987 Generation and manipulation of uniform mean shear with the use of screens. *Exps Fluids* **5**, 247.

LAUNDER, B. E., REECE, G. J. & RODI, W. 1975 Progress in the development of a Reynolds stress turbulence closure. *J. Fluid Mech.* **68**, 537.

LUMLEY, J. L. 1978 Computational modeling of turbulent flows. *Adv. Appl. Mech.* **18**, 123.

MOIN, P., ROGERS, M. M. & MOSER, R. D. 1985 Structure of turbulence in the presence of uniform shear. *Proc. 5th Symp. Turb. Shear Flows, Ithaca*, p. 1.

MULHEARN, P. J. & LUXTON, R. E. 1975 The development of turbulence structure in a uniform shear flow. *J. Fluid Mech.* **68**, 577.

NAOT, D., SHAVIT, A. & WOLFSHTEIN, W. 1973 Two point correlation model and the redistribution of Reynolds stresses. *Phys. Fluids* **16**, 738.

REIS, F. B. 1952 Studies of correlation and spectra in homogeneous turbulence. Ph.D. dissertation, Massachusetts Institute of Technology.

ROBERTSON, J. M. & JOHNSON, H. F. 1970 Turbulence structure in plane Couette flow. *J. Engng Mech. Div. ASCE* **96**, 1171.

RODI, W. 1976 A new algebraic relation for calculating the Reynolds stresses. *Z. Angew. Math. Mech.* **56**; 219.

ROGALLO, R. S. 1981 Numerical experiments in homogeneous turbulence. *NASA TM*-81315.

ROGALLO, R. S. & MOIN, P. 1984 Numerical simulation of turbulent shear flows. *Ann. Rev. Fluid Mech.* **16**, 99.

ROHR, J. J., ITSWEIRE, E. C., HELLAND, K. N. & VAN ATTA, C. W. 1988 An investigation of the growth of turbulence in a uniform shear flow. *J. Fluid Mech.* **187**, 1.

ROSE, W. G. 1966 Results of an attempt to generate a homogeneous turbulent shear flow. *J. Fluid Mech.* **25**, 97.

ROSE, W. G. 1970 Interaction of grid turbulence with a uniform mean shear. *J. Fluid Mech.* **44**, 767.

ROTTA, J. 1951 Statistische theorie nichthomogener turbulenz. *J. Phys.* **129**, 547.

SHAANAN, S., FERZIGER, J. H. & REYNOLDS, W. C. 1977 Numerical simulation of turbulence in the presence of shear. *Dept. Mech. Engng, Stanford University, Rep.* TF-6.

SREENIVASAN, K. R. 1985 The effect of contraction on a homogeneous turbulent shear flow. *J. Fluid Mech.* **154**, 187.

SREENIVASAN, K. R., TAVOULARIS, S., HENRY, R. & CORRSIN, S. 1980 Temperature fluctuations and scales in grid-turbulence. *J. Fluid Mech.* **100**, 597.

TAVOULARIS, S. 1985 Asymptotic laws for transversely homogeneous turbulent shear flows. *Phys. Fluids* **28**, 999.

TAVOULARIS, S. & CORRSIN, S. 1981*a* Experiments in a nearly homogeneous shear flow with a uniform mean temperature gradient. Part 1. *J. Fluid Mech.* **104**, 311.

TAVOULARIS, S. & CORRSIN, S. 1981*b* Experiments in nearly homogeneous turbulent shear flow with a uniform mean temperature gradient. Part 2. The fine structure. *J. Fluid Mech.* **104**, 349.

TCHEN, C. M. 1953 On the spectrum of energy in turbulent shear flow. *Natl Bur. Stand. J. Res.* 50 res. Pap. 2388.

TOWNSEND, A. A. 1976 *The Structure of Turbulent Shear Flow.* Cambridge University Press.

WEINSTOCK, J. & BURK, S. 1985 Theoretical pressure–strain term, experimental comparison, and resistance to large anisotropy. *J. Fluid Mech.* **154**, 429.